Korean J. Chem. Eng., 32(4), 650-660 (2015)
DOI: 10.1007/s11814-014-0276-z

pISSN: 0256-1115
eISSN: 1975-7220

A study on the removal of heavy metals and anionic dyes from aqueous solution by amorphous polyamide resin containing chlorobenzalimine and thioamide as chelating groups

Thangaraj Vidhyadevi*, Murugesan Arukkani*, Kalaivani Selvaraj*, Premkumar Manickam Periyaraman*, Ravikumar Lingam, and Sivanesan Subramanian*,†**

*Department of Applied Science and Technology, AC Tech, Anna University, Chennai 600 025, India
**Department of Chemistry, C.B.M. College, Affiliated to Bharathiar University, Coimbatore 641 042, India
(*Received 20 March 2014 • accepted 14 September 2014*)

Abstract−Poly(chlorobenzalimino thiourea amide) (PCBA) resin was synthesized by using the phosphorilation poly condensation method. PCBA was characterized by analytical techniques, and it was used for the adsorption of heavy metals (Ni^{2+} and Zn^{2+}) and anionic dyes (methyl orange (MO) and acid orange (AO)). The variables which affect the adsorption efficiency, such as pH, adsorbate concentration, adsorbent dose and contact time were studied. The results show that the adsorption of Ni^{2+}, Zn^{2+}, MO and AO follows the pseudo-second order kinetic model. The maximum monolayer adsorption capacity of PCBA for Ni^{2+}, Zn^{2+}, MO and AO, calculated using Langmuir isotherm is 191.2, 247.1, 153.8, 149 mg/g, respectively. Surface area (21.1 m^2/g) and crystal size are 21.1 m^2/g and 0.35 nm, respectively. High efficiency of the polymeric resins may be due to their amorphous nature and the presence of strong binding sites in the polymer structure. Thermodynamic parameters such as change in standard free energy change, enthalpy and entropy ΔG^o, ΔH^o and ΔS^o were evaluated, and the adsorption process was found to be feasible, exothermic and spontaneous. Desorption studies show that adsorption efficiency of PCBA was retained even after four cycles.

Keywords: Polyamides, Azomethine, Thiourea, Isotherm, Desorption

INTRODUCTION

Environmental contamination with heavy metal ions is a serious problem due to their tendency to accumulate in living organism and toxicities in relatively low concentration [1,2]. Wastewater containing complex dye molecules presents a serious disposal problem. The various treatment processes available for the removal of metals and dyes are adsorption, membrane separation, coagulation-flotation; advanced oxidation, reverse osmosis etc. Among them, adsorption is a popular technique in recent years, due to its efficiency in removal of the pollutants. Activated carbon is one of the most widely used adsorbents for this purpose [3-5]. However, activated carbon still suffers from costly regeneration. Even though activated carbon is well recognized and widely used, adsorption capacities, mechanical strength need further improvement [6-8]. In the past few years, polymeric adsorbents have been emerging as potential alternative to activated carbon in terms of their vast surface area, perfectly mechanical rigidity, adjustable surface chemistry, pore size distribution, and feasible regeneration under mild condition. Polymeric adsorbents such as divinylbenzene crosslinked polystyrene without any chelating group are mainly used for the removal of organic chemicals such as aniline, phenol, and dichloro methane, benzene [9-11]. In these types of adsorbents, the adsorption affinity between adsorbate and adsorbent is relatively weak due to the absence of other specific interaction. Consequently, efficient removal of a given pollutant by these adsorbents needs further improvement. As a result, chemically modified polymeric adsorbents were developed. In such polymeric adsorbents, a polymeric matrix like polystyrene is chemically modified to have chelating function groups such as tertiary amine [12], sulfonic [13], dicarboxylbenzoyl [14] and amino [15] groups for the removal of organic and metal ion pollutants. In the recent years, polymeric chelating adsorbents have been tailor-made to selectively adsorb toxic heavy metals from industrial streams and other aqueous systems. Such adsorbents generally consist of two sections: the polymeric matrix and the immobilized chelating groups. Polymeric chelating adsorbents are selectively used for various targeted heavy metal ions like Cu [16], Ni [17], Zn [18], and Cr [19]. However, the immobilized chelating groups are restricted to a few groups like ethylenediamine [20], acetic acid [17], and glycene groups [21]. An alternative and easier approach to this restriction is to incorporate selective and desirable chelating groups into the polymer backbone itself during polymer synthesis. In this method, there is no need for immobilization of chelating groups. Recently, our group has made attempts in synthesizing novel polymeric adsorbents in which chelating groups are inherently bound to the polymer backbone. Novel adsorbents of this type such as, poly(phenylthiourea)imine [22], polyazomethineamides [23], and polyamides [24] have been found to be more efficient for the removal of Zn^{2+}, Ni^{2+}, Pb^{2+}, Cu^{2+} and Cd^{2+}, respectively from aqueous solutions.

The aim of the present study was to synthesize and characterize novel amorphous polyamides with azomethine and thioamide

†To whom correspondence should be addressed.
E-mail: sivanesh1963@gmail.com

binding sites and to study their adsorption capacity for the removal of metal ions (Ni^{2+} and Zn^{2+}) as well as anionic dyes (AO and MO). The effects of pH, initial adsorbate concentration, adsorbent dose and contact time on the adsorption of metals and dyes were investigated. Kinetic and equilibrium models were used to determine the adsorption mechanism of metals and dyes on PCBA, and to calculate of the adsorption capacity of PCBA respectively. Desorption studies were carried out to study the regeneration of PCBA.

MATERIALS AND METHODS

1. Chemicals and Reagents

Chlorobenzaldehyde (Fluka), 2-aminoterephthalic acid (Aldrich), diaminobiphenyl sulfone (Aldrich), triphenylphosphite (Fluka), ammoniumthiocyanate (Fluka) dimethyl formamide (DMF) (Himedia), pyridine (Qualigens), ethanol (Aldrich), hydrochloric acid (Qualigens), nitric acid (Qualigens), acetic acid (Qualigens), sodium hydroxide (Qualigens) were used as such or otherwise purified according to the standard procedures. $NiSO_4 \cdot 6H_2O$, $ZnSO_4 \cdot 7H_2O$, methyl orange and acid orange were procured from Sigma-Aldrich Chemical, India.

2. Adsorbent Synthesis

Poly(azomethine thioamide) was synthesized by the direct phosphorilation polycondensation method, using dicarboxylic acid monomer and 4,4′-bis(thiourea)biphenylsulphone. The dicarboxylic acid monomer, 2-(p-chlorobenzalimino)terephthalic acid containing azomethine group was synthesized by condensing 0.01 mol of chlorobenzaldehyde and 0.01 mol of 2-aminoterephthalic acid in DMF (50 mL), with pyridine (2 mL) as the catalyst at 110 °C for 4 h. 2.5 mmol of acid monomer, 2.5 mmol of the 4,4′-bis(thiourea)biphenylsulphone, 5.2 mmol of triphenylphosphite and 6-10 mmol of pyridine were mixed and kept at temperatures around 140 °C in a DMF solvent for 4 h. The reaction mixture was cooled to room temperature, and poured into ethanol to precipitate the polymer. It was then filtered and washed with 5% HCl, 5% $NaHCO_3$ to remove the unreacted monomer. It was then washed with distilled water, and finally with ethanol, dried under a vacuum pump, and used as an adsorbent for the removal of Ni^{2+}, Zn^{2+}, MO and AO. The structure of PCBA is shown in Fig. 1.

3. Adsorbates

$NiSO_4 \cdot 6H_2O$, $ZnSO_4$, methyl orange and acid orange were purchased from Sigma Aldrich Chemical, India. The metal and dye stock solutions were prepared by dissolving a suitable amount of the metal salts and dyes in distilled water. Before mixing the adsorbent, the pH of each test solution was adjusted to the required value with 0.1 N NaOH or 0.1 N HCl. The initial and final concentrations of the metal and dye solutions were analyzed by the flame atomic absorption spectrometer (Shimadzu, Japan), and a double

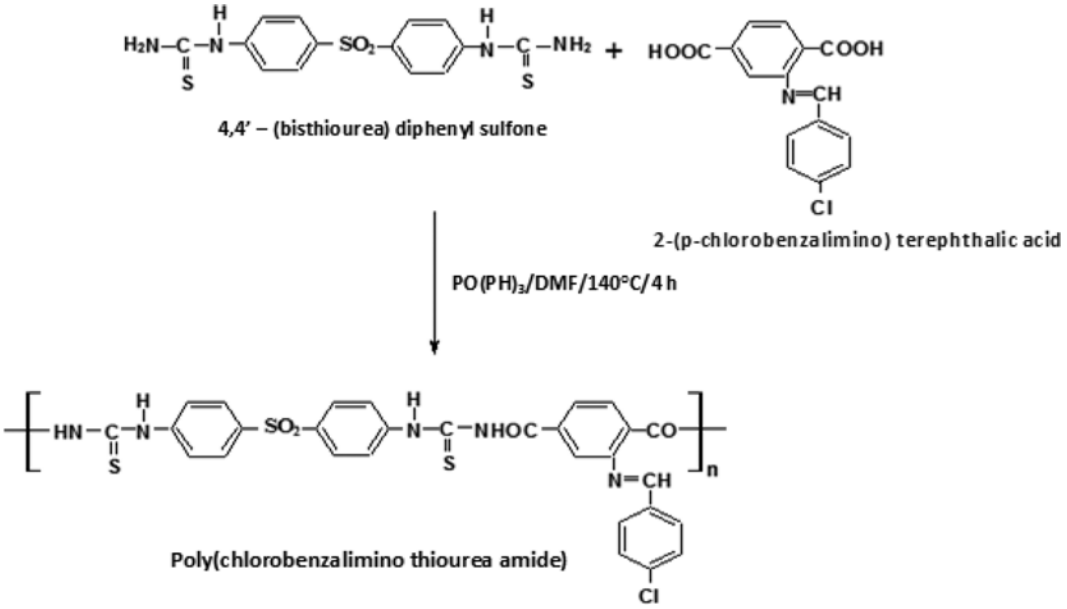

Fig. 1. Scheme-I.

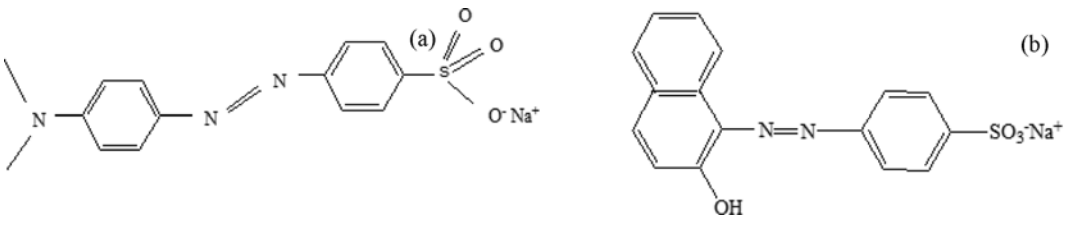

Fig. 2. Structure of (a) methyl orange and (b) acid orange.

beam UV spectrophotometer (Shimadzdu, Japan) respectively. The structure of the MO and AO dyes is shown in Fig. 2(a) and 2(b) respectively. The UV visible spectra of MO and AO dye solutions during adsorption were determined in the wavelength range of 525 nm and 483 nm respectively.

4. Analytical Method

The synthesized PCBA was characterized by the Fourier transform infrared spectroscopy (FTIR), nuclear magnetic resonance spectroscopy (NMR), thermo gravimetric analysis (TGA), X-Ray diffraction analysis (XRD) and scanning electron microscopic (SEM) techniques. The functional groups in the polymer were identified using the KBr pellet technique in a Perkin-Elmer FT-IR spectrometer, in the spectral range of 4,000 to 650 cm^{-1}. The H^1 NMR spectrum of the polymer was recorded in DMSO-d_6 using the Bruker Instrument. The thermal analysis was under static air atmosphere at a heating rate of 10 °C/min using the Perkin-Elmer analyzer. The specific surface area was determined by BET-N_2 adsorption, using the Micromeritics instrument (model ASAP 2020). The crystalline nature and crystal size were calculated using the XRD analysis (Seifert make, ISO Debyeflex-2002 model, Germany). The surface morphology of the polymer before and after adsorption was obtained by using the Leo Gemini 1530 scanning electron microscope (SEM), at an accelerating voltage of 10 kV and at a working distance of 20 μm.

5. Batch Experiments

Batch adsorption experiments were performed in 250 mL conical flasks containing 20 mL of 50 mg/L adsorbate solution with 40 mg of PCBA. The pH of the solution was maintained at 6 (for Ni^{2+} and Zn^{2+}) and at 4 (for MO and AO) and these flasks were agitated on a horizontal bench shaker (Orbitek) for 60 min (in case of metal ions) and for 100 min (in case of dyes). The mixtures were centrifuged to separate the adsorbent and the solutions were analyzed by the respective spectrometer. The extent of adsorption at equilibrium (mg g^{-1}) was calculated using the following relationship:

$$q_e = \frac{C_o - C_e}{W} \times V \quad (1)$$

where C_o and C_e are the initial and final adsorbate concentrations (mg/L), V is the volume of the adsorbate solution (mL), and W is the mass of the adsorbent (mg).

6. Equilibrium Isotherm

20 mL of each of the metal and dye solutions were taken in separate 250 mL conical flasks with a predetermined initial concentration (25-300 mg/L). 40 mg of PCBA was added to each flask, and the pH of the solution was maintained at 6 (for Ni^{2+} and Zn^{2+}) and at 4 (for MO and AO). The flasks containing metal ions were agitated for 60 min, and the flasks containing dyes were agitated for 100 min. Then the mixture was centrifuged to separate the adsorbent and the solutions were analyzed in the respective spectrometers.

7. Kinetic Studies

For kinetic studies, 40 mg of PCBA was taken with 20 mL of the adsorbate solution of a known concentration (50 mg/L). An optimum pH of 6 was maintained for the Ni^{2+} and Zn^{2+} ions solution, and pH 4 was fixed for MO and AO dye solution experiments. The concentration of the adsorbate in the aqueous solution was determined at different contact times (20-160 min). The solutions were centrifuged and analyzed as mentioned before.

8. Thermodynamic Studies

The effect of temperature on metal and dye adsorption experiments was evaluated at different temperatures (in °C) of 30, 40, 50 and 60. This study was performed with initial adsorbate concentration of 50 mg/L, PCBA dose of 40 mg, contact time of 60 min for metal ions and 100 min for dyes and the pH of the solution was maintained at 6 (for Ni^{2+} and Zn^{2+}) and at 4 (for MO and AO).

9. Desorption Studies

The recovery and reusability of the spent adsorbent is an essential parameter in adsorption technology. In this study, metal loaded (Ni^{2+} and Zn^{2+}) PCBA was kept in 100 mL of 2 N HCl for about 1.5 h, and then washed with plenty of water. The dyes (MO and

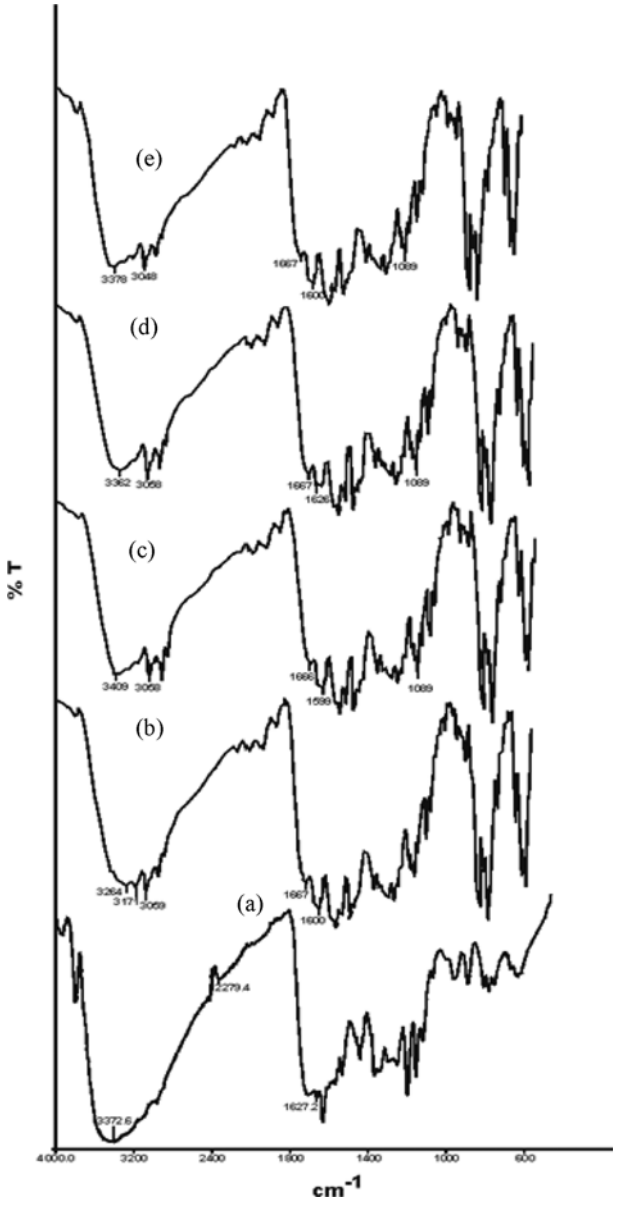

Fig. 3. FT-IR spectrum of (a) PCBA (b) Ni^{2+} treated PCBA, (c) Zn^{2+} treated PCBA, (d) MO treated PCBA and (e) AO treated PCBA.

AO) under study are acidic in nature, and exhibit good affinity towards the basic medium; therefore, an aqueous solution of 100 mL of NaOH (2 N) is capable of eluting the dyes from PCBA in 2 h. The metal ion/dye desorbed PCBA was used as adsorbent for the further adsorption cycles.

RESULTS AND DISCUSSION

1. Characterization of PCBA

The IR Spectrum of poly(azomethine thioamide) is shown in Fig. 3(a). In the polymer PCBA, the amide -NH , amide (I) -C=O and amide (II) -N-C=O frequencies appeared at 3,372, 1,672 and 1,594 cm^{-1} respectively. The imine -CH stretching frequency appeared at 2,279 cm^{-1} (Fig. 3(a)). Since the -CH=N- stretching frequency also falls in the same region of that of carbonyl stretching frequency of the amide link, it appeared as a shoulder at 1,627 cm^{-1}. There are significant changes in the FT-IR spectra of the metal ion/dye adsorbed polymers when compared to that of raw polymer (PCBA) (Fig. 3(b) to Fig. 3(e)). The shape of the carbonyl stretching frequency and -CH=N- stretching frequency has undergone significant changes. The -CH=N- stretching frequency of the polymer shifted to a lower value of 1,599-1,600 cm^{-1}. This clearly indicates that the -CH=N- groups are probable binding sites. Moreover, the imine -CH stretching frequency appeared at 2,279 cm^{-1} in the polymer has completely disappeared in the metal ion/dye adsorbed polymers. The shape and -NH bending frequency of the polymer has also undergone changes when compared to the metal ion/dye adsorbed polymers, which is an indication that the amide link in the polymer is also involved in the adsorption of metal ions and dyes.

The ^{1}H NMR spectrum of PCBA is shown in Fig. 4. The peak at δ=10.8 ppm is due to the amide proton, and that of the -CH=N- proton appeared at δ=8.2 ppm. The complex aromatic region of the polyamide appeared as a broad signal in the region δ=7.9-6.1 ppm.

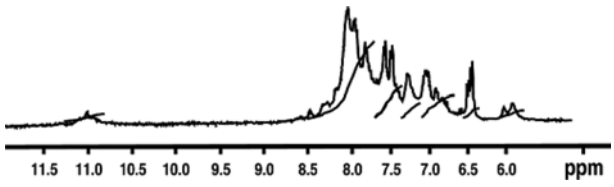

Fig. 4. ^{1}H- NMR spectrum of PCBA.

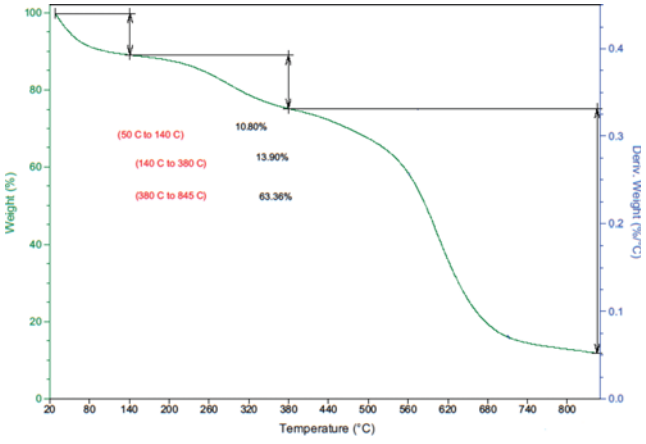

Fig. 5. TGA curve of PCBA.

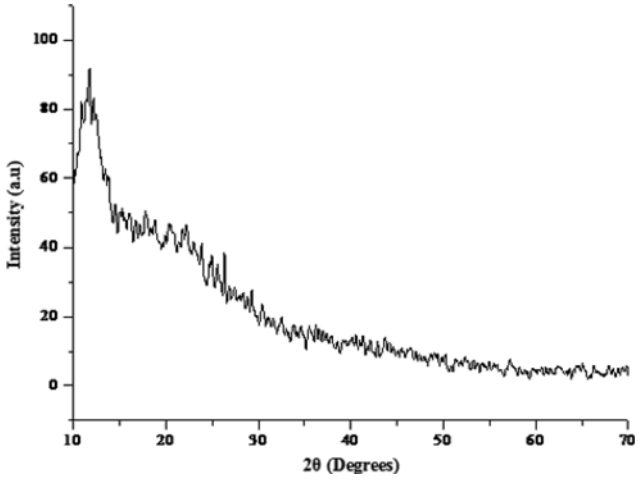

Fig. 6. XRD pattern of PCBA.

The thermal stability of PCBA was examined by TGA and the results are shown in Fig. 5. PCBA undergoes three stages of degradation. The first weight loss (10.80%) was observed in the temperature range of 50 to 140 °C, which may be due to the evaporation of the occluded solvent and moisture. The second (13.90%) and the third weight losses (63.36%) occurred in the region of 140 to 380 °C and 380 to 845 °C, respectively. The second weight loss was due to internal moisture evaporation. The final weight loss was due to the decomposition of the PCBA polymer. This result shows that PCBA possesses good thermal stability.

The surface area of PCBA was measured by nitrogen adsorption at 150 °C. The samples were degassed at 150 °C for 12 h. The surface area of the PCBA was found to be 21.12 m^2/g, which shows that PCBA has considerable surface area towards adsorption of Ni^{2+}, Zn^{2+}, MO and AO.

The X-ray diffraction patterns are shown in Fig. 6. A broad peak (2θ=11.65) was observed in the wide angle X-ray diffraction intensity curve, with less intensity indicating the absence of crystallinity in PCBA. The particle size of the PCBA was calculated using the Scherrer formula [25].

$$\text{Crystal size} = \frac{k \times \lambda}{\beta \times \cos\theta} \quad (2)$$

where k=constant (0.9), λ=X-ray wavelength (1.54 Å), β=full width at half maximum (FWHM) measured in radians (0.4), and θ=the angle of the peak position (5.82). The calculated PCBA crystallite size is 0.35 nm. This implies that PCBA has a smaller grain size and is almost amorphous.

Figs. 7(a), (b), (c), (d) and (e) show the surface morphology of PCBA before and after adsorption. From Fig. 7(a), it is clear that PCBA has a considerable number of porous sites, which indicates a good possibility for the adsorption of metals and dyes. Fig. 7(b), (c), (d) and (e) show that after adsorption, the porous surface of the PCBA gets filled by metal ions (Ni^{2+} and Zn^{2+}) and dye (MO and AO) molecules.

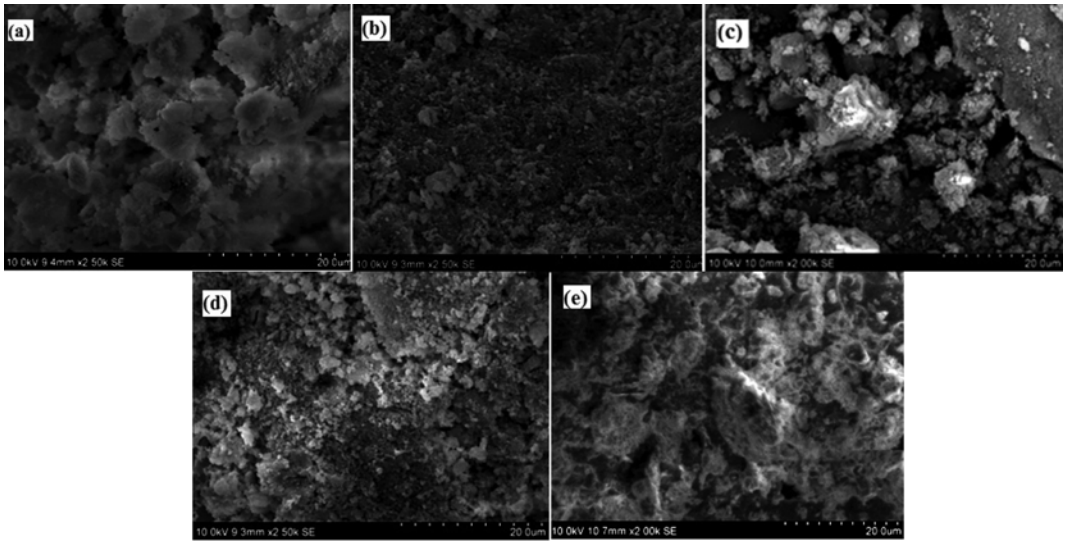

Fig. 7. (a) SEM images of (a) PCBA, (b) Ni^{2+}, (c) Zn^{2+}, (d) MO (e) AO treated PCBA.

2. Batch Adsorption Studies

The effect of pH on the percentage removal of metals and dyes was determined in the pH range of 3 to 9. This study was performed with initial adsorbate concentration of 50 mg/L, PCBA dose of 40 mg, contact time of 60 min for metal ions and 100 min for dyes. From Fig. 8(a), the maximum percentage of adsorption for Ni^{2+} and Zn^{2+} ions appears to occur at pH 6. Similarly, the maximum removal of MO and AO occurs at pH 4.

The point of zero charge pH_{zpc} of PCBA was found to be 4.38. The adsorption system is strongly pH dependent, which could be explained by the zero charge pH_{zpc} of PCBA and the different functional groups (present in PCBA) which are involved in the binding. At lower pH (<5), the protons and metal cations (Ni^{2+} and Zn^{2+}) compete with each other for binding onto PCBA, and hence there is less removal. Moreover, the adsorption of cations is favored at $pH>pH_{zpc}$, whereas, the adsorption of anions is favored at $pH<pH_{zpc}$

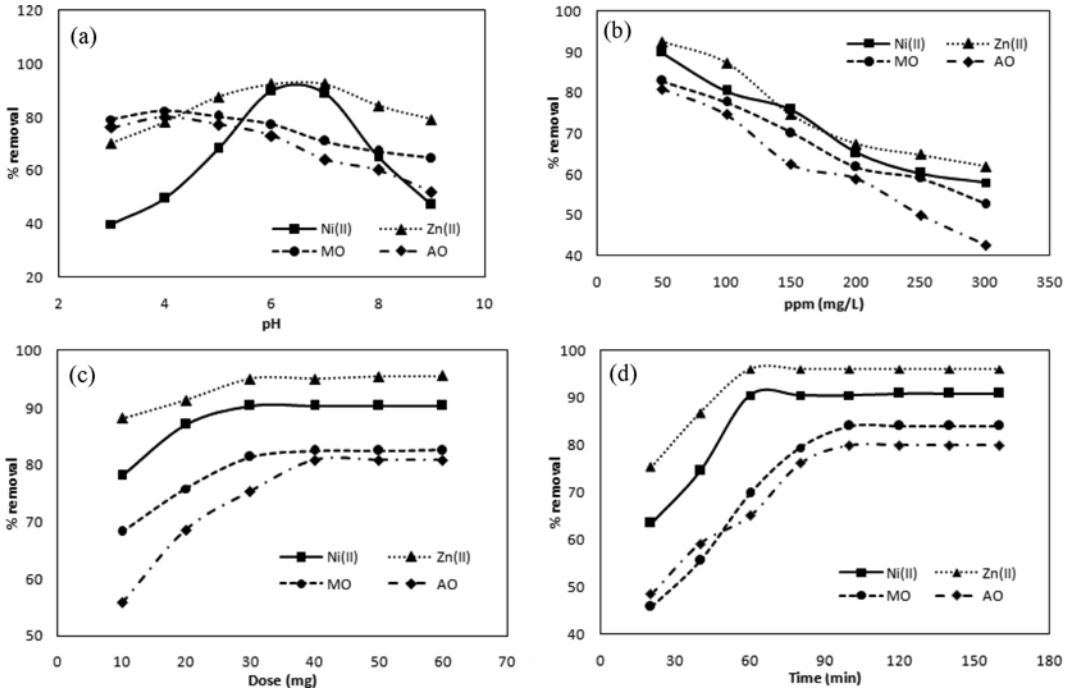

Fig. 8. (a) Effect of pH (initial adsorbate concentration 50 mg/L, dose=40 mg, time=60 min for Ni^{2+}, Zn^{2+} ions & 100 min for MO and AO), (b) effect of concentration (pH=6 for Ni^{2+}, Zn^{2+} ions & 4 for MO and AO, dose=40 mg, time=60 min for Ni^{2+}, Zn^{2+} ions & 100 min for MO and AO), (c) adsorbent dose (pH=6 for Ni^{2+}, Zn^{2+} ions & 4 for MO and AO, initial adsorbate concentration 50 mg/L, time= 60 min for Ni^{2+}, Zn^{2+} ions & 100 min for MO and AO) and (d) effect of contact time (pH=6 for Ni^{2+}, Zn^{2+} ions & 4 for MO and AO, initial adsorbate concentration 50 mg/L, dose=40 mg) on adsorption of Ni^{2+}, Zn^{2+}, MO and AO over PCBA.

[26]. At higher pH, dye anions and OH^- compete with each other, and hence the removal of dyes was less. From the above results, an optimum pH of 6 was fixed for the Ni^{2+} and Zn^{2+} adsorption experiments, and an optimum pH of 4 was fixed for further MO and AO adsorption experiments.

Fig. 8(b) shows the percentage removal of metals and dyes as a function of the initial adsorbate concentration. The experiments were performed at different initial adsorbate concentrations in the range of 25-300 mg/L, PCBA dose of 40 mg and the pH of the solution was maintained at 6 (for Ni^{2+} and Zn^{2+}) and at 4 (for MO and AO). It can be seen that the percentage removal decreases with an increase in the adsorbate concentration, because there is an increase in competition for active adsorption sites. At higher concentrations more metal ions and dye molecules are left unadsorbed, due to the saturation of the binding sites. But the amount of the adsorbate adsorbed per unit weight of the adsorbent increases with an increases in the initial adsorbate concentration (not shown). This increase in the adsorption capacity of PCBA may be due to the utilization of more active sites for adsorption at a higher adsorbate concentration.

The PCBA dose is an important parameter in batch adsorption studies, as it determines the adsorption capacity of PCBA, which may be attributed to the availability of more binding sites and increased surface area. This experiment was performed to ascertain the effect of adsorbent dose on the uptake of the metal ions and dyes. Adsorbent doses ranging from 10 to 60 mg in 20 mL of 50 mg/L of adsorbate solutions were taken. The pH of the solution was maintained at 6 (for Ni^{2+} and Zn^{2+}) and at 4 (for MO and AO). The percentage removal of the Ni^{2+}, Zn^{2+} ions, MO and AO increases (Fig. 8(c)) with an increase in the PCBA dose initially and thereafter remains constant. Since the active sites were filled up at an adsorbent dose of 40 mg, further addition of the adsorbent would not produce any considerable change in the percentage removal. So the optimum adsorbent dose of 40 mg was fixed for other adsorption studies.

The effects of the contact time on the adsorption of metal ions (Ni^{2+} and Zn^{2+}) and dyes (MO and AO) are shown in Fig. 8(d). The experiment was performed for a given adsorbate concentration of 50 mg/L and fixed adsorbent dose of 40 mg. The pH of the solution was maintained at 6 (for Ni^{2+} and Zn^{2+}) and at 4 (for MO and AO). It can be observed that the adsorption rate increases with an increase in the contact time in the beginning, and then gradually slows down, until equilibrium is reached. The maximum removal of metal ions was attained in 60 min, and for dyes it was 100 min. This may be because a large surface area is available in the initial stages of adsorption. Beyond a particular time, no further adsorption takes place, because most of the adsorption sites are occupied.

3. Kinetic Models

Kinetic models were used to describe the mechanism of adsorption and rate controlling steps, to evaluate the adsorption kinetics of metal ions and dyes. Three kinetic models, namely, pseudo-first order, pseudo-second order and intra-particle diffusion, were applied to the experimental data.

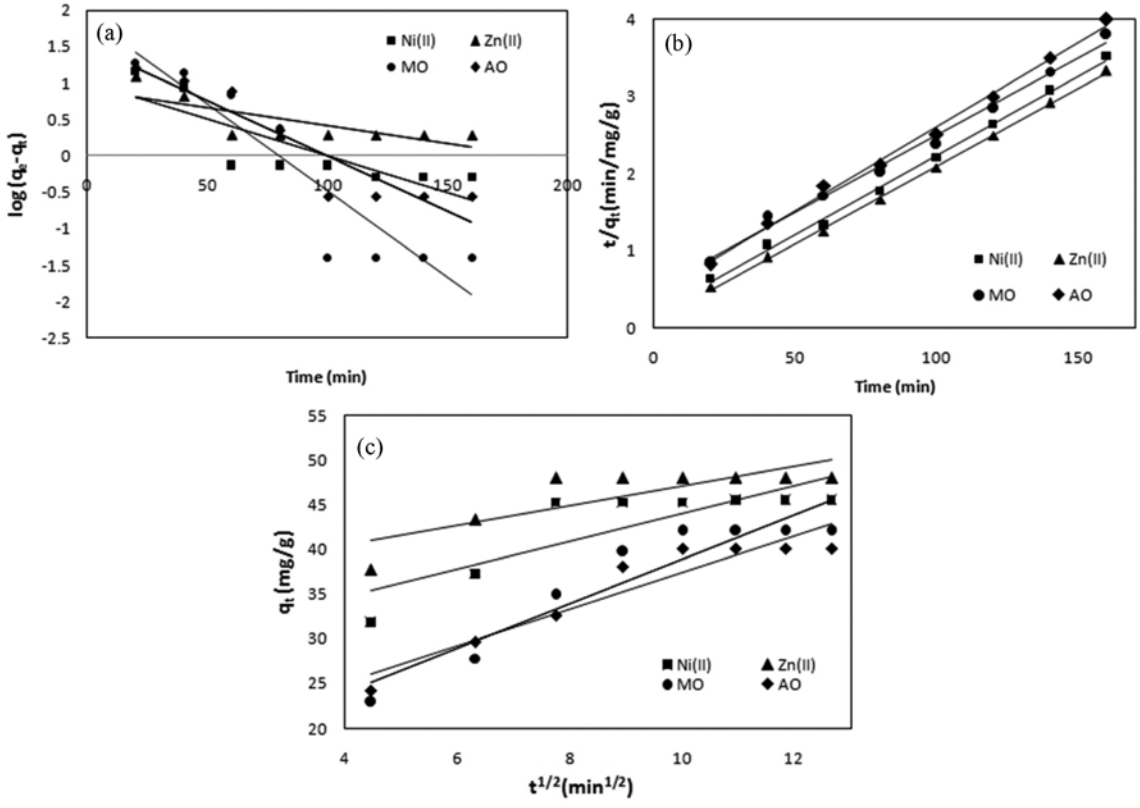

Fig. 9. (a) Pesudo-first order model, (b) Pseudo-second order model (c) Intra particle diffusion model for adsorption of Ni^{2+}, Zn^{2+}, MO and AO on PCBA (pH=6 for Ni^{2+}, Zn^{2+} ions & 4 for MO and AO, initial adsorbate concentration 50 mg/L, dose=40 mg).

Table 1. Kinetic models constants for adsorption of Ni^{2+}, Zn^{2+}, MO and AO onto PCBA (pH=6 for Ni^{2+}, Zn^{2+} ions & 4 for MO and AO, initial adsorbate concentration=50 mg/L, PCBA dose=40 mg)

Kinetic model	Parameters	Metal ion solution		Dye solution	
		Ni^{2+} ion	Zn^{2+} ion	MO dye	AO dye
Pseudo-first order	K_1 (min^{-1})	0.02303	0.01128	0.05481	0.035
	$q_{e,cal}$ (mg/g)	10.0253	7.9726	80.4452	33.4503
	R^2	0.6868	0.5858	0.8524	0.8664
Pseudo-second order	$q_{e,cal}$ (mg/g)	48.54	49.75	49.75	45.66
	k_2 (g mg^{-1} min^{-1})	2.432×10^{-3}	4.122×10^{-3}	0.8205×10^{-3}	1.1465×10^{-3}
	h (mg g^{-1} min^{-1})	5.711	10.204	2.0386	2.3906
	$q_{e,exp}$ (mg/g)	46	50	42.1	40.3
	R^2	0.997	0.999	0.9918	0.9949
Intra particle diffusion model	k_{ad} (mg/g·$min^{1/2}$)	1.5687	1.1065	2.5074	2.045
	C	28.365	36.076	13.582	16.921
	R^2	0.7097	0.6719	0.8792	0.892

The Lagergren pseudo-first order [27] model is given as,

$$\log(q_e - q_t) = \log q_e - \frac{k_1}{2.303}t \quad (3)$$

where q_e and q_t are the amount of adsorbates adsorbed on PCBA (mg/g) at equilibrium and at time t respectively, and k_1 (min^{-1}) is the rate constant of the pseudo-first order equation. The rate constant (k_1) and q_e are calculated from the slope and intercept of the graph drawn between $\log(q_e - q_t)$ versus t (Fig. 9(a)), listed in Table 1.

The pseudo-second order equation [28] is

$$\frac{t}{q_t} = \frac{1}{k_2 q_e^2} + \frac{t}{q_e} \quad (4)$$

where k_2 is the rate constant for the second order model (g mg^{-1} min^{-1}), and $h=k_2q_e^2$ is the initial adsorption rate (mg $g^{-1}min^{-1}$). The values of q_e and k_2 are calculated from the slope and intercept of the plot between t/q_t and t (Fig. 9(b)).

Intraparticle diffusion explains the mechanism and the step affecting the kinetics of adsorption. According to this model, the solid-liquid interaction can be explained by three different steps. The first region indicates the removal of adsorbate from the bulk solution to the external surface of PCBA. The second region corresponds to the particle diffusion, where, adsorbate moves to the interior of PCBA. The third portion corresponds to the adsorption of adsorbate on the interior surface of the pores of PCBA [29].

The intraparticle diffusion [30] during the adsorption process is defined by the equation,

$$q_t = k_{ad}t^{1/2} + C \quad (5)$$

where k_{ad} is the intraparticle diffusion rate constant (mg·$g^{-1}min^{-1/2}$), and intercept 'C' is the boundary layer effect. The larger the intercept, the greater is the boundary layer effect. A plot of q_t versus $t^{1/2}$ (Fig. 9(c)) gives a straight line and does not pass through the origin. If the plot passes through the origin, intraparticle diffusion is the only rate limiting step [31]. However, in this study, the linear plots for metal ion/dye did not pass through the origin. Such a deviation from origin indicates that intraparticle diffusion is not a rate limiting step. All the kinetic model constants are listed in Table 1.

The correlation coefficient values (R^2) obtained from the pseudo-first order kinetic model and intra particle diffusion models are very low for metal and dye adsorption, and the maximum deviation is observed between the calculated and experimental q_e values (in case of pseudo-first order). This indicates that the pseudo-first order kinetic model could not explain the adsorption mechanism of metal ions and dyes on PCBA. In the case of the pseudo-second order model, the R^2 values are higher for the adsorption of metal ions and dyes, when compared with other experimental data. In addition, the calculated q_e values are also closer to the experimental q_e values. Therefore, it can be inferred that the adsorption of Ni^{2+}, Zn^{2+}, MO and AO can be well represented by the pseudo-second order kinetic model.

4. Adsorption Isotherm

Fig. 10(a)-(d) shows the adsorption isotherm of Ni^{2+}, Zn^{2+}, MO and AO onto PCBA, respectively. In this study, three different non-linear isotherm models, namely, the Langmuir, Freundlich, and Temkin are discussed.

The Langmuir model [32] assumes the Langmuir equation is based on the assumption of a structurally homogenous adsorbent, where all adsorption sites are identical and energetically equivalent. This indicates that the adsorption occurs until a monolayer of adsorption is completed, and after that completion no more interaction between the adsorbent and adsorbate molecules takes place.

The Langmuir non-linear isotherm model is expressed as

$$q_e = \frac{q_m k_L C_e}{1 + k_L C_e} \quad (6)$$

where q_m (mg/g) and k_L are the maximum adsorption capacity and Langmuir constant, and C_e (mg/L) is the concentration of the adsorbate solution at equilibrium.

The dimensionless constant R_L is the essential characteristic of the Langmuir isotherm and it can be expressed as,

$$R_L = \frac{1}{1 + k_L C_0} \quad (7)$$

The values of R_L imply whether the adsorption is favorable ($0<R_L<1$) or unfavorable ($R_L>1$) or linear ($R_L=1$) or irreversible ($R_L=0$).

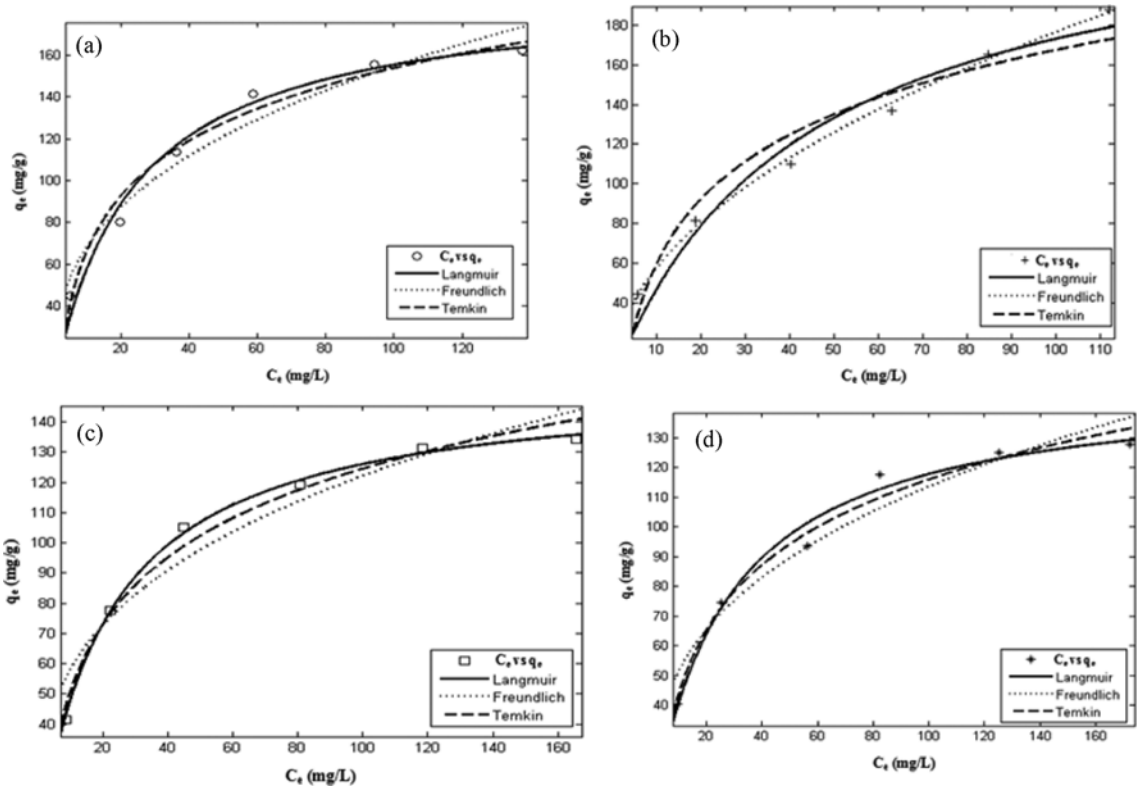

Fig. 10. Non-linear adsorption isotherm for (a) Ni^{2+} adsorption, (b) Zn^{2+} adsorption, (c) MO adsorption and (d) AO adsorption onto PCBA (pH=6 for Ni^{2+}, Zn^{2+} ions & 4 for MO and AO, dose=40 mg, time=60 min for Ni^{2+}, Zn^{2+} ions & 100 min for MO and AO).

The Freundlich non-linear equation [33] assumes that adsorption occurs on a heterogeneous surface having unequally available sites with different binding energies. It can be described as,

$$\log q_e = \log k_F + \frac{1}{n}\log C_e \quad (8)$$

where k_F is the Freundlich constant indicating the adsorption capacity, and it represents the quantity of the adsorbate adsorbed on the adsorbent for unit equilibrium concentration. The values of 1/n represent the favorability of the adsorption process (0<1/n<1).

The Temkin non-linear isotherm [34] describes the heat of adsorption and adsorbate-adsorbent interaction on the surface. It is commonly applied in the following form:

$$q_e = B\ln(AC_e) \quad (9)$$

where A is the Temkin isotherm constant (L/g) and B=(RT)/b, 'b' is the Temkin constant related to the heats of adsorption, R is the universal gas constant (8.314 J/mol·K) and 'T' is the temperature in Kelvin.

The R_L values of Nickel (0.316-0.071), Zinc (0.461-0.125), methyl orange (0.3057-0.069) and acid orange (0.347-0.082) indicate that the adsorption process is favorable. All the isotherm experimental data were fitted to isotherm models using MATLAB 7.8 and the graphical representation of these models is represented in Fig. 10(a)-(d).

Table 2 gives the isotherm parameters for the Langmuir, Freundlich and Temkin isotherms. Based on the correlation coefficient values (R^2), the Langmuir isotherm gives the best fit when compared to the other isotherm models. This implies that monolayer adsorption takes place on PCBA for metals (Ni^{2+} and Zn^{2+}) and dyes (MO and AO). The maximum monolayer adsorption capacity values of PCBA for Ni^{2+}, Zn^{2+}, MO and AO as calculated from the Langmuir isotherm are 191.2, 247.1, 153.8, 149 mg/g, respectively. The comparison of the maximum monolayer adsorption capacity of Ni^{2+}, Zn^{2+}, MO and AO onto various adsorbents is represented in Table 3. It shows that PCBA studied in this work has good adsorption capacity when compared with other adsorbents.

Table 2. Isotherm Parameters for the adsorption of Ni^{2+}, Zn^{2+}, MO and AO over PCBA (pH=6 for Ni^{2+}, Zn^{2+} ions & 4 for MO and AO, dose=40 mg, time=60 min for Ni^{2+}, Zn^{2+} ions & 100 min for MO and AO)

Isotherm model	Parameters	Ni^{2+} ion	Zn^{2+} ion	MO dye	AO dye
Langmuir	K (L/mg)	0.0433	0.0234	0.04543	0.0371
	q_m (mg/g)	191.2	247.1	153.8	149
	R^2	0.9982	0.9609	0.9978	0.9838
Freudlich	K_f (mg/g)	18.62	30.01	27.57	23.37
	n	20.48	2.806	3.094	2.914
	R^2	0.9959	0.9567	0.9327	0.9427
Temkin	α (L/mg)	0.5715	0.3577	0.4851	0.3995
	β (mg^{-1})	16.51	20.33	13.93	13.65
	R^2	0.9767	0.9483	0.9838	0.9800

Table 3. Comparison of adsorption capacity of different adsorbents for the removal of Ni^{2+}, Zn^{2+}, MO and AO from aqueous solutions

Adsorbent	Adsorption capacity (mg/g)				References
	Ni^{2+} ion	Zn^{2+} ion	MO dye	AO dye	
Chelax-100	0.126	-	-	-	[17]
PGLY chelating resin	0.063	-	-	-	[21]
Natural Clinoptilolite	11.44	-	-	-	[35]
Orange peel	62.89	-	-	-	[36]
Cashew nut shell	18.868	-	-	-	[37]
Physic seed hull	-	12.29	-	-	[38]
Cashew nut shell	-	24.98	-	-	[39]
Azardirachata India black	-	33.49	-	-	[40]
Canola stalks	-	-	24.8	-	[41]
TiO_2 nano tube	-	-	137	-	[42]
Granular activated carbon	-	-	125	-	[43]
Cellulose-based wastes	-	-	-	21.0	[44]
Surfactant modified silica gel	-	-	-	47.17	[45]
Hyper cross linked polymeric adsorbent	-	-	-	70.9	[46]
PCBA	191.2	247.1	153.8	149	Present study

5. Adsorption Thermodynamics

Thermodynamic studies of an adsorption process are necessary to determine whether a process will occur spontaneously or not. Thermodynamic parameters such as free energy (ΔG^o), enthalpy (ΔH^o) and entropy (ΔS^o) change of adsorption can be evaluated from the following Eqs. ((10)-(13)) [47]:

$$K_a = \frac{q_e}{C_e} \tag{10}$$

$$\Delta G^o = -RT\ln K_c \tag{11}$$

$$\Delta G^o = \Delta H^o - T\Delta S^o \tag{12}$$

$$\log K_a = \frac{\Delta S^o}{2.303R} - \frac{\Delta H^o}{2.303RT} \tag{13}$$

where K_a is the equilibrium constant (L/mg), q_e is the solid phase concentration at equilibrium (mg/g) and C_e is the liquid phase concentration at equilibrium (mg/L). ΔG^o, ΔH^o and ΔS^o are changes in

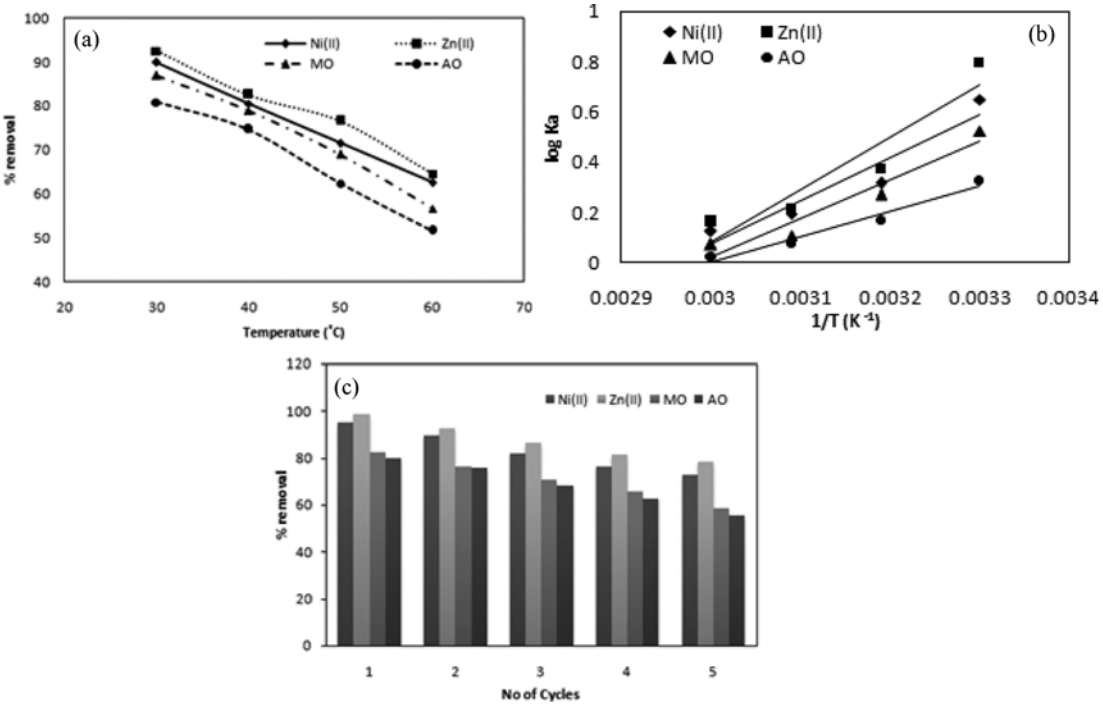

Fig. 11. (a) Effect of temperature (pH=6 for Ni^{2+}, Zn^{2+} ions & 4 for MO and AO, initial adsorbate concentration 50 mg/L, dose=40 mg, time=60 min for Ni^{2+}, Zn^{2+} ions & 100 min for MO and AO), (b) plot of log Kc versus 1/T for adsorption of Ni^{2+}, Zn^{2+}, MO and AO on PCBA c) Recyclability of PCBA.

Table 4. Thermodynamic parameters for adsorption of Ni^{2+}, Zn^{2+}, MO and AO onto PCBA (pH=6 for Ni^{2+}, Zn^{2+} ions & 4 for MO and AO, initial adsorbate concentration=50 mg/L, PCBA dose=40 mg, time=60 min for Ni^{2+}, Zn^{2+} ions & 100 min for MO and AO)

Parameters	Temperature (K)	Metal ion solution		Dye solution	
		Ni^{2+} ion	Zn^{2+} ion	MO dye	AO dye
$-\Delta H^o$ (kJ·mol^{-1})		32.74	39.88	29.37	19.15
$-\Delta S^o$ (kJ·mol^{-1})		96.79	118.06	87.67	57.40
$-\Delta G^o$ (kJ·mol^{-1})	303	3.78	4.16	2.75	1.71
	313	1.89	1.96	1.43	0.88
	323	1.22	1.11	0.58	0.41
	333	0.82	0.87	0.39	0.13

Gibbs free energy (kJ/mol), enthalpy (kJ/mol) and entropy (J/mol/K), respectively. R is the gas constant (8.314 J/mol/K), T is the temperature (K). The values of ΔH^o and ΔS^o are determined from the slope and the intercept of the plots of log K_a versus 1/T (Fig. 11(b)). The ΔG^o values were calculated from the thermodynamic experimental values using Eq. (11). Percentage removal of Ni^{2+}, Zn^{2+}, MO and AO on PCBA decreased when the temperature was increased from 303 to 333 K is shown in Fig. 11(a). The calculated values of thermodynamic parameters are given in Table 4. The negative ΔG^o at different temperatures indicates the spontaneous nature of the adsorption of Ni^{2+}, Zn^{2+}, MO and AO onto the PCBA. The negative ΔH^o value suggests the exothermic nature of the process; it would be expected that the increase in temperature would result in an increase in adsorption capacity and the negative ΔS^o can describe the randomness at the PCBA-solution interface during the adsorption of Ni^{2+}, Zn^{2+}, MO and AO onto the PCBA. Similar results have been published by other researchers [48,49].

6. Desorption Studies

Metal loaded (Ni^{2+} and Zn^{2+}) PCBA was kept in 2 N HCl for about 1.5 h, and then washed with plenty of water. The dyes (MO and AO) under study are acidic in nature, and exhibit good attraction towards the basic medium. An aqueous solution of NaOH (2 N) is capable of eluting the dyes from PCBA. The regenerated PCBA was reused for up to four adsorption cycles, and the results are given in Fig. 11(c). From this figure, it is clear that the adsorption efficiency of the PCBA drops a little after each cycle. This might be due to the ignorable amount of the PCBA lost during the adsorption process.

CONCLUSION

This study indicates that PCBA is a suitable adsorbent for the removal of heavy metals (Ni^{2+}, Zn^{2+}) and dyes (MO and AO). Different functional groups like amide carbonyl, azomethine, amide and thioamide groups are present in the polymer backbone, which are responsible for the maximum adsorption capacity of PCBA. The maximum adsorption of metals Ni^{2+} (89.96%) and Zn^{2+} (92.58%) by PCBA occurs at pH 6. Similarly, the optimum pH for the maximum removal of anionic dyes (MO (82.51%) and AO (80.21%)) by PCBA is 4. The kinetic results suggest that the adsorption process occurs by the pore diffusion mechanism. Desorption studies show that adsorption using PCBA is a reversible process. Thus, PCBA has high adsorption capacity and it could be used as an alternative adsorbent for the adsorption Ni^{2+}, Zn^{2+} ions, MO and AO. It is concluded that, PCBA can be used for the removal of industrial effluents containing Ni^{2+}, Zn^{2+} ions, MO and AO.

ACKNOWLEDGEMENT

One of the authors (Ms. T. Vidhyadevi) is thankful to the Council of Scientific and Industrial Research (CSIR), Govt. of India, New Delhi, for providing fellowship during the work done.

REFERENCES

1. B. J. Nepal and R. T. Wright, *Environmental Science*, Fifth Ed., Prentice-Hall, Inc., New Jersy, 348 (1996).
2. C. Y. Chen, C. L. Chiang and C. R. Chen, *Sep. Purif. Technol.*, **54**, 396 (2007).
3. S. Karaca, A. Gurses, A. Acikyildiz and M. Ejder, *Micropor. Mesopor. Mater.*, **115**, 376 (2008).
4. Z. Yu, S. Peldszus and P. M. Huck, *Water Res.*, **42**, 2873 (2008).
5. Y. Safa, H. N. Bhatti, I. A. Bhatti and M. Asgher, *Can. J. Chem. Eng.*, **89**, 1554 (2011).
6. O. Hernandez-Remirez and S. M. Holmes, *J. Mater. Chem.*, **18**, 2751 (2008).
7. S. S. Tripathy and A. M. Raichur, *J. Hazard. Mater.*, **153**, 1043 (2008).
8. T. A. Johnson, N. Jain, H. C. Joshi and S. Prasad, *J. Sci. Ind. Res.*, **67**, 647 (2008).
9. V. V. Azanova and J. Hradil, *React. Funct. Polym.*, **41**, 163 (1999).
10. J.-W. Lee, H.-J. Jung, D.-H. Kwak and P.-G. Chung, *Water Res.*, **39**, 617 (2005).
11. E. J. Simpson, R. K. Abukhadra, W. J. Koros and R. S. Schechter, *Ind. Eng. Chem. Res.*, **32**, 2269 (1993).
12. C.-F. Chang, C.-Y. Chang, K.-E. Hsu, S.-C. Lee and W. Höll, *J. Hazard. Mater.*, **155**, 295 (2008).
13. A. M. Li, J. Fan, W. B. Yang, J. G. Cai, X. Zhang, J. Y. Zhou, Q. X. Zhang, C. Long, F. Q. Liu and Q. X. Zhang, Chinese Patent, CN1858007A (2006).
14. N. Masque, M. Galia and R. M. Marce, *Chromotographia.*, **50**, 21 (1999).
15. B. L. Rivas, S. A. Pooley, H. A. Maturana and S. Villegas, *J. Appl. Polym. Sci.*, **80**, 2123 (2001).
16. M. V. Dinu and E. S. Dragan, *React. Funct. Polym.*, **68**, 1346 (2008).
17. H. Leinonen and J. Lehto, *React. Funct. Polym.*, **43**, 1 (2000).
18. H. P. Schneider and U. Wallbaum, US Patent, 4,895,905 (1990).
19. K. O. Saygi, M. Tuzen, M. Soylak and L. Elci, *J. Hazard. Mater.*, **153**,

1009 (2008).
20. A. Nastasović, S. Jovanović, D. Đorđević, A. Onjia, D. Jakovljević and T. Novaković, *React. Funct. Polym.*, **58**, 139 (2004).
21. H. Leinonen and J. Lehto, *React. Funct. Polym.*, **43**, 1 (2000).
22. C. Y. Chen, C. Y., C. L. Chiang and C. R. Chen, *Sep. Purif. Technol.*, **54**, 396 (2007).
23. A. Murugesan, T. Vidhyadevi, S. S. Kalaivani, M. P. Premkumar, L. Ravikumar and S. Sivanesan, *Chem. Eng. J.*, **197**, 368 (2012).
24. A. Murugesan, L. Ravikumar, V. SathyaSelvaBala, P. SenthilKumar, T. Vidhyadevi, S. D. Kirupha, S. S. Kalaivani, S. Krithiga and S. Sivanesan, *Desalination*, **271**, 199 (2011).
25. S. Dinesh Kirupha, A. Murugesan, T. Vidhyadevi, P. Baskaralingam, S. Sivanesan and L. Ravikumar, *Sep. Sci. Technol.*, **48**, 254 (2013).
26. M. J. Mas-Guindal, E. Benko and M. A. Rodríguez, *J. Alloys Compd.*, **454**, 352 (2008).
27. S. Lagergren, *Kungliga Sven. Vetensk Handl.*, **24**, 1 (1898).
28. Y. S. Ho and G. McKay, *Process Biochem.*, **34**, 451 (1999).
29. G. McKay, *J. Chem. Technol. Biotechnol.*, **33A**, 196 (1983).
30. W. J. Weber and J. C. Morris, *J. Sanit. Eng. Div. Am. Soc. Civ. Eng.*, **89**, 31 (1963).
31. C. Theivarasu, S. Mylsamy and N. Sivakumar, *Res. J. Chem. Sci.*, **1**(7), 38 (2011).
32. I. Langmuir, *J. Ame. Chem. Soc.*, **40**, 1361 (1918).
33. H. M. F. Freundlich, *J. Phys. Chem.*, **57**, 385 (1906).
34. M. J. Temkin and V. Pyzhev, *Act. Physicochim. URSS*, **12**, 217 (1940).
35. R. Nevenka, S. Djordje, J. Mina, N. Z. Logarc, M. Mazajc and V. Kaucicc, *Appl. Surf. Sci.*, **257**, 1524 (2010).
36. F. Gonen and D. D. Serin, *Afr. J. Biotechnol.*, **11**(5), 1250 (2012).
37. P. SenthilKumar, V. Ramalingam, S. Dinesh Kirupha, A. Murugesan, T. Vidhyadevi and S. Sivanesan, *Chem. Eng. J.*, **167**, 122 (2011).
38. M. Mohammad, S. Maitra, N. Ahmad, A. Bustam, T. K. Sen and B. K. Dutta, *J. Hazard. Mater.*, **179**, 363 (2010).
39. P. SenthilKumar, S. Ramalingam, R. V. Abhinaya, S. D. Kirupha, T. Vidhyadevi and S. Sivanesan, *Can. J. Chem. Eng.*, **90**, 973 (2012).
40. P. King, K. Anuradha, S. B. Lahari, Y. P. Kumar and V. S. R. K. Prasad, *J. Hazard. Mater.*, **152**, 324 (2008).
41. Y. Hamzeh, S. Izadyar, E. Azadeh, A. Abyaz and Y. Asadollahi, *Iran. J. Environ. Health Sci. Eng.*, **4**(1), 49 (2011).
42. S. Xu, J. Ng, X. Zhang, H. Bai and D. D. Sun, *Colloids Surf., A.*, **379**, 169 (2011).
43. O. SoonAn, E. Toorisaka, M. Hirata and T. Hano, *J. Environ. Sci.*, **20**, 952 (2008).
44. G. Annadurai, R.-S. Juang and D.-J. Lee, *J. Hazard. Mater.*, **92**, 263 (2002).
45. S. Koner, B. K. Saha, R. Kumar and A. Adak, *Int. J. Current. Res.*, **33**(6), 128 (2011).
46. J. H. Huang, K. L. Huang, S. Q. Liu, A. T. Wang and C. Yan, *Colloids Surf. A.*, **330**, 55 (2008).
47. J. He, S. Hong, L. Zhang, F. Gan and Y. S. Ho, *Fresen. Environ. Bull.*, **19**(11), 2651 (2010).
48. A. Murugesan, T. Vidhyadevi, S. S. Kalaivani, M. P. Premkumar, L. Ravikumar and S. Sivanesan, *Chem. Eng. J.*, **197**, 368 (2012).
49. J. Goscianska, M. Marciniak and R. Pietrzak, *Chem. Eng. J.*, **247**, 258 (2014).